P. Song
Graduate Student,
e-mail: pengs@grip.cis.upenn.edu

P. Kraus
Graduate Student,
e-mail: pkraus@grip.cis.upenn.edu

V. Kumar
e-mail: kumar@grip.cis.upenn.edu
Mem. ASME

GRASP Laboratory,
University of Pennsylvania,
3401 Walnut Street,
Philadelphia, PA 19104

P. Dupont
Department of Aerospace and
Mechanical Engineering,
Boston University,
Boston, MA 02215
e-mail: pierre@bu.edu
Mem. ASME

Analysis of Rigid-Body Dynamic Models for Simulation of Systems With Frictional Contacts

The use of Coulomb's friction law with the principles of classical rigid-body dynamics introduces mathematical inconsistencies. Specifically, the forward dynamics problem can have no solutions or multiple solutions. In these situations, compliant contact models, while increasing the dimensionality of the state vector, can resolve these problems. The simplicity and efficiency of rigid-body models, however, provide strong motivation for their use during those portions of a simulation when the rigid-body solution is unique and stable. In this paper, we use singular perturbation analysis in conjunction with linear complementarity theory to establish conditions under which the solution predicted by the rigid-body dynamic model is stable. We employ a general model of contact compliance to derive stability criteria for planar mechanical systems. In particular, we show that for cases with one sliding contact, there is always at most one stable solution. Our approach is not directly applicable to transitions between rolling and sliding where the Coulomb friction law is discontinuous. To overcome this difficulty, we introduce a smooth nonlinear friction law, which approximates Coulomb friction. Such a friction model can also increase the efficiency of both rigid-body and compliant contact simulation. Numerical simulations for the different models and comparison with experimental results are also presented. [DOI: 10.1115/1.1331060]

1 Introduction

There are many applications in an industrial setting where it is beneficial to understand the dynamics of systems with frictional contacts. Examples include part-feeding systems ([1]) and automatic assembly of mechanical components ([2]). Examples of mechanical systems with frictional contacts include multifingered grippers ([3]), multiarm manipulation systems ([4]), legged locomotion systems, and wheeled robots on uneven terrain ([5]). In order to successfully design and optimize such mechanical systems or manufacturing processes, a method for modeling and simulating mechanical systems with frictional contacts is necessary ([6]).

In a forward dynamics problem, it is well known that in the frictionless case there is always a unique solution for the accelerations. When the constraints are not all independent, the system is statically indeterminate and the constraint forces cannot be uniquely determined. In the frictional case, if all contacts are known to be rolling (sticking), the existence of a solution can be shown if the constraints are independent ([7]). In all other cases, the initial value problem can be shown to have no solution or multiple solutions for special choices of initial conditions ([8,9]). The major difficulty of proving existence and uniqueness arises when rigid-body models are combined with friction laws coupling normal and tangential contact forces. In these situations, it is attractive to pursue models in which the contact forces are explicit functions of the state variables. For example, a continuum model for modeling the deformations at each contact is described in ([10]). Each contact is modeled as frictional elastic or viscoelastic, and the contact force distribution across the contact patch is calculated using a finite element mesh. This general approach is further refined by [11]. Existence and uniqueness is shown for the special case in which the maximum tangential force at each point is a priori known.

The empirical nature of friction models can cause additional difficulties with dynamic simulation. The most widely employed model, for example, is Coulomb friction. When used in combination with a rigid-body contact model, the tangential force is a discontinuous function of the sliding velocity and independent of tangential displacement. Furthermore, this model does not predict such phenomena as microslip, hysteresis, and local adhesion ([12]). Both these difficulties can be overcome by combining the Coulomb friction model with a simple lumped model of compliance (e.g., the Kelvin-Voigt model [13]). At very small displacements, the tangential force opposes the tangential displacement, simulating an approximately linear spring. For small oscillatory displacements, hysteric behavior is exhibited as in [14]. With a suitable modification to the Coulomb friction model, the steady-state friction force can be made to decrease with increasing velocity thus simulating the development of a lubricant film ([12]). However, while the difficulty with discontinuities is eliminated, such Coulomb-like friction laws are generally not smooth. The laws are described by separate equations for rolling and sliding contact and are not differentiable at transitions between rolling and sliding. We will overcome this difficulty by introducing a friction model that depends on normal force, but which is continuously differentiable.

In this paper, we derive a simple *compliant contact model* that (a) provides a framework for analyzing frictional forces for constraint dynamic systems; and (b) establishes a unique solution for initial value problems in dynamic simulation. We use methods from singular perturbation analysis to establish conditions under which the solution predicted by the rigid-body model is *stable*. We argue that rigid-body dynamic simulation is meaningful only when the solution of the compliant contact model converges to the solution of the rigid-body model. Experimental results and numerical simulations are illustrated to verify the stability analysis. We also describe stability results using a *smooth nonlinear friction law* which is an alternative to the Coulomb's friction model.

2 Rigid-Body Models

The dynamic equations of motion for a mechanical system comprised of rigid bodies subject to Coulomb friction can be written in the form

$$M(q)\ddot{q} + h(q,\dot{q}) = u + \Phi_q^T \lambda \tag{1}$$

where $q \in \mathfrak{R}^n$ is the vector of generalized coordinates, $M(q)$ is an $n \times n$ positive-definite symmetric inertia matrix, $h(q,\dot{q})$ is a $n \times 1$ vector of nonlinear inertial forces, u is the vector of applied (external) forces and torques, and λ is the vector of constraint forces. The system is subject to k unilateral constraints:

$$\Phi(q) = (\phi_1(q), \cdots, \phi_k(q))^T \geq 0 \tag{2}$$

and Φ_q in Eq. (1) is the $k \times n$ Jacobian matrix, $\partial\Phi/\partial q$. We will assume, without loss of generality, that this does not include bilateral, holonomic constraints. Further, for the sake of simplicity, we will assume that nonholonomic constraints are not present.

Suppose there are c contacts, consisting of r rolling contacts and s sliding contacts. Let the subscripts N and T denote quantities in the normal and tangential contact directions and the subscripts S and R denote sliding and rolling contacts, respectively. The Jacobian matrix and constraint forces in Eq. (1) are given by

$$\Phi_q^T = (\dot{\Phi}_{S_q}^T \Phi_{NR_q}^T \Phi_{TR_q}^T), \quad \dot{\Phi}_{S_q}^T = (\Phi_{NS_q}^T + \Phi_{TS_q}^T \mu_s), \tag{3}$$

$$\lambda = (\lambda_{NS}^T \lambda_{NR}^T \lambda_{TR}^T)^T, \tag{4}$$

where $\mu_s = -\text{diag}(\mu \, \text{sign}(\Phi_{TS}))$, μ is a $s \times s$ diagonal matrix that contains all the coefficients of friction at the sliding contacts, $\dot{\Phi}_{S_q}$ is a $s \times n$ matrix, Φ_{NR_q} and Φ_{TR_q} are both $r \times n$ matrices, and the total number of constraints $k = 2r + s$. λ_{NS} is the s-dimensional vector of normal forces at sliding contacts, while λ_{NR} and λ_{TR} are the $r \times 1$ vectors of normal and tangential forces at rolling contacts, respectively.

Contacts between rigid bodies generate complementary constraints on the position (or velocity or acceleration) variables and the corresponding force variables. In the normal direction, if no new contact becomes active over a finite time interval, then in that interval, there is a complementary equation satisfied by the relative normal acceleration, $\ddot{\phi}_{N,i}$, and the normal force, $\lambda_{N,i}$ ([8])

$$\ddot{\phi}_{N,i} \geq 0, \quad \lambda_{N,i} \geq 0, \quad \ddot{\phi}_{N,i}\lambda_{N,i} = 0, \quad i = 1, \ldots, c. \tag{5}$$

This complementary constraint is valid for all sliding contacts (indexed by the subscript $i = 1, \ldots, s$) and rolling contacts (indexed by $i = s+1, \ldots, c$). Subscripts R and S are omitted for convenience. This condition allows active contacts to become inactive. The case of inactive contacts becoming active is modeled by rigid-body impacts and is treated elsewhere ([13]). Similar

complementarity constraints can be found in the tangential direction by assuming Coulomb's friction. We refer the reader to ([15]) for details.

The problem of determining contact forces can be reduced to a linear complementarity problem (LCP) that has the form ([7])

$$x \geq 0, \quad y = Ax + B > 0, \quad y^T x = 0. \tag{6}$$

The LCP has a unique solution for all vectors B if an only if the matrix A is a P matrix ([16]). However, even if A is not a P matrix, the LCP may have unique solution for special choices of B. For other choices of B, Eq. (6) may have no solution or multiple solutions. To overcome these inconsistencies, we consider more sophisticated models of contact interactions in the next section.

3 Compliant Contact Models

Our contact model of compliance assumes that the principles of rigid-body dynamics are valid and the gross motion of the dynamic system is described by the state variables $(q,\dot{q})$. However, in addition to the gross motion, there are small (local) deformations at each contact. Thus a rigid body can be modeled as a rigid core surrounded by a very thin deformable layer the inertia of which is considered to be negligible, as shown in the schematic in Fig. 1. The gross rigid-body motion determines the relative displacement at the contact point (ϕ_T, ϕ_N). The actual relative displacement of the contact point is given by $(\phi_T + \delta_T, \phi_N + \delta_N)$. The contact forces are related to the normal and tangential deformations (δ_N, δ_T) of the deformable layer and their derivatives $(\dot{\delta}_N, \dot{\delta}_T)$ through the material properties of the deformable layer.

A general viscoelastic model for contact compliance is shown in Fig. 1. At contact i, the normal and tangential contact forces $(\lambda_{N,i}$ and $\lambda_{T,i})$ between the two contacting bodies may be modeled as

$$\lambda_{N,i} = f_{N,i}(\delta_{N,i}) + g_{N,i}(\delta_{N,i}, \dot{\delta}_{N,i}), \quad i = 1, \ldots, c, \tag{7}$$

$$\lambda_{T,i} = f_{T,i}(\delta_{T,i}) + g_{T,i}(\delta_{T,i}, \dot{\delta}_{T,i}), \quad i = 1, \ldots, c, \tag{8}$$

where the functions $f_{N,i}$ and $f_{T,i}$ are the elastic stiffness terms and $g_{N,i}$ and $g_{T,i}$ are the damping terms in the normal and tangential directions, respectively. These functions depend on the geometry and material properties of the two bodies in contact and may be nonlinear. We have decoupled the modeling of the contact forces (i.e., the force at a contact is only dependent on the deformation at that contact). We will consider the case where the tangential force obeys Coulomb's frictional law:

$$|\lambda_{T,i}| \leq \mu_i \lambda_{N,i}. \tag{9}$$

An alternative frictional model is discussed in Section 7.
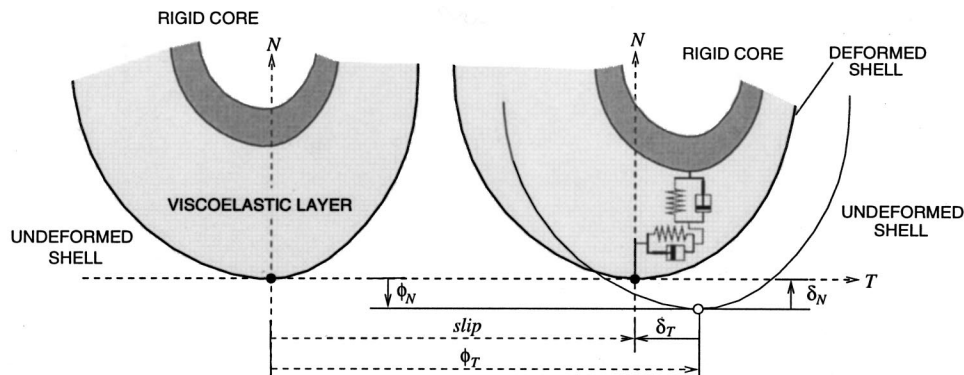
Fig. 1   A simple model of contact compliance

The simplest viscoelastic model is the Kelvin-Voigt model given by

$$f_i = K_i \delta_i, \quad g_i = C_i \dot{\delta}_i, \quad i = 1, \ldots, c, \qquad (10)$$

where K_i and C_i are stiffness and damping coefficients (in the normal or tangential directions) respectively. The coefficients can be estimated using linear elastic and viscoelastic theory for half-spaces ([17]). A more sophisticated model due to Hunt and Crossley ([18]) incorporates nonlinear elastic and dissipation terms:

$$f_i = K_i \delta_i^\beta, \quad g_i = \frac{3}{2} \alpha K_i \delta_i^\beta \dot{\delta}_i, \quad i = 1, \ldots, c, \qquad (11)$$

where α and β are functions of the material properties and the local geometry.

In any of the above models, the normal deformations are directly related to the constraints in the normal direction. The normal deformations and constraint forces are given by

$$\delta_{N,i} = \max\{0, -\phi_{N,i}(q)\}, \qquad (12)$$

if $\delta_{N,i} > 0$,

$$\begin{cases} \dot{\delta}_{N,i} = -\dot{\phi}_{N,i}(q), \quad i = 1, \ldots, c \\ \lambda_{N,i} = \max\{0, f_{N,i}(\delta_{N,i}) + g_{N,i}(\delta_{N,i}, \dot{\delta}_{N,i})\}. \end{cases} \qquad (13)$$

In the tangential direction we define a new variable, σ_i, to denote the relative sliding velocity between the (deformed) contact points at contact i. This quantity is the *slip rate*, the sum of the tangential rigid-body velocity at the contact and the rate of tangential deformation:

$$\sigma_i = \dot{\phi}_{T,i} + \dot{\delta}_{T,i}.$$

For rolling contacts, we have

$$\lambda_{T,i} = f_{T,i}(\delta_{T,i}) + g_{T,i}(\delta_{T,i}, \dot{\delta}_{T,i}) \qquad (14)$$

$$\dot{\delta}_{T,i} = -\dot{\phi}_{T,i}(q), \quad i = s+1, \ldots, c, \qquad (15)$$

in conjunction with the frictional inequality of Eq. (9). For sliding contacts,

$$\dot{\delta}_{T,i} = h_{T,i}(\lambda_{T,i} - f_{T,i}(\delta_{T,i})), \qquad (16)$$

$$\lambda_{T,i} = -\mu \lambda_{N,i} \text{sign}(\sigma_i), \quad i = 1, \ldots, s, \qquad (17)$$

where $h_{T,i}(.)$ is the inverse of the function $g_{T,i}$ in Eq. (8) for a given $\delta_{T,i}$. For both sliding and rolling contacts, we track the tangential deformations by integrating the expression for its derivative:

$$\delta_{T,i} = \int_{t_0}^t \dot{\delta}_{T,i} dt + \delta_{T,i}(t_0). \qquad (18)$$

In order to determine which set of equations apply, we start with the assumption that any contact is rolling. If the tangential force from Eq. (15) violates the frictional constraint in (9), the contact is sliding and Eqs. (16)–(17) yield the correct force with sign(σ_i) taken to be the opposite of the sign of the tangential force in Eq. (15). It is clear that Eqs. (12)–(18) always provide a unique answer for the normal and tangential contact forces and the positive-definiteness of M in Eq. (1) yields a unique solution for $\ddot{q}$.

There are two disadvantages of the compliant contact model. First it is clear that we now need to model the contacts and this increases the possibility of modeling errors. Second, and more importantly from an computational standpoint, there is a need to extend the dimension of the state space from $2n - 2(c+r)$ to $2n + c$ in order to track the tangential deformation, $\delta_{T,i}$, at each contact. The three main advantages, which outweigh the disadvantages, are: (a) The normal and tangential forces are now uniquely determined and there is no question of static indeterminacy; (b) The difficulties with uniqueness and existence no longer arise; and

(c) A model with tangential contact compliance is more realistic and can better explain physical observations ([13]).

We do not wish to promote unnecessary model complexity, however, and in those situations when a compliant contact model is not needed, it would be desirable to retain the simpler rigid-body model. The popularity of rigid-body models can be attributed not only to their simplicity, but also to the fact that they produce adequate results in a broad range of applications. Clearly, rigid-body models can only be used when a unique solution can be determined without any additional ad hoc assumptions. But even when this is the case, it is meaningful to use the reduced-order rigid-body model only when the solution from the more accurate compliant contact model converges to the solution obtained from the rigid-body model. In the next section, we will use singular perturbation theory to investigate the *stability* of the solutions obtained from the rigid-body model.

4 Singular Perturbation Analysis

The rigid-body model leads to a set of differential-algebraic equations as shown in Section 2. In the compliant contact model, the deformations at the contact points are at least an order of magnitude smaller than the gross motions of the mechanical system. By setting these small deformations to zero (or by allowing the corresponding stiffnesses to be infinitely large), we recover the equations of the rigid-body model. This suggests that we can use singular perturbation theory to decompose the system model into reduced (slow time scale) and boundary layer (fast time scale) models ([19]). In mechanical systems described by Eq. (1), the slow time scale corresponds to the reduced-order rigid-body model dynamics and the fast time scale is the time scale that characterizes the contact dynamics ([20,21]). The response of the system then consists of a slow response and a fast transient. If the boundary layer model is exponentially stable, the fast transient will exponentially converge to zero and it is reasonable to neglect the high-frequency contact dynamics. In such a situation, the reduced-order model obtained by neglecting the compliance is robust to the unmodeled dynamics. If the boundary layer model is not stable, we cannot neglect these terms and it is necessary to use the complete dynamic model given by Eqs. (12)–(18).

We first partition the generalized coordinates q into the fast variables q_1, related to the contact deformations, and the remaining slow variables, q_2. We accordingly define a new set of variables:

$$p = \begin{pmatrix} p_1 \\ p_2 \end{pmatrix} = \begin{pmatrix} \Phi_N(q_1, q_2) \\ \Phi_{TR}(q_1, q_2) \\ q_2 \end{pmatrix} \in \mathfrak{R}^n,$$

where $p_1, q_1 \in \mathfrak{R}^k$ and $p_2, q_2 \in \mathfrak{R}^{n-k}$. Recall that k is the total number of constraints. In order to make p a valid choice of coordinates, the implicit function theorem requires that the Jacobian matrix

$$\Gamma = \begin{pmatrix} \Phi_{Nq(c \times n)} \\ \Phi_{TRq(r \times n)} \\ 0_{(n-k) \times k} \quad I_{(n-k) \times (n-k)} \end{pmatrix} \in \mathfrak{R}^{n \times n}$$

be nonsingular, that is, the contact normals and the rolling tangents have to be linearly independent. If these conditions are satisfied, we may write

$$\begin{pmatrix} \dot{q}_1 \\ \dot{q}_2 \end{pmatrix} = J(p_1, p_2) \begin{pmatrix} \dot{p}_1 \\ \dot{p}_2 \end{pmatrix}$$

where $J = \Gamma^{-1}$. Note that the choice of the p-coordinates is arbitrary as long as Γ^{-1} exists. The time variable and the p-coordinates can be nondimensionalized by letting

$$\bar{t} = \frac{t}{T}, \quad \bar{p}_1 = D_1^{-1} p_1, \quad \bar{p}_2 = D_2^{-1} p_2, \qquad (19)$$

where T is the characteristic time scale and $\bar{t}$ is dimensionless. $\bar{p}_1$ and $\bar{p}_2$ are the nondimensionalized fast and slow variables, respectively. D_1 is a diagonal matrix whose components are the deformation length scales while D_2 is a diagonal matrix of the characteristic scales of the slow variables. For the sake of simplicity, all contacts are assumed to have similar physical properties, and the diagonal matrix of the deformation scales can be defined as $D_1 = d_1 \cdot I_{k \times k}$. We also define a parameter ϵ as the dimensionless ratio, d_1/L, where L is the length scale for gross rigid-body

motions. As d_1 tends to zero, ϵ goes to zero, and the compliant contact model degenerates into the rigid-body model.

We use ϵ and the dimensionless variables in (19) to perform a second change of coordinates. Let

$$\mathbf{x} = (x_1, x_2)^T = (\bar{p}_2, \bar{p}_2')^T, \quad \mathbf{y} = (y_1, y_2)^T = (\bar{p}_1, \sqrt{\epsilon}\bar{p}_1')^T \quad (20)$$

be the new state variables and rewrite the dynamic Eqs. (1) in state space notation:

$$\begin{pmatrix} \sqrt{\epsilon}y_1' \\ x_1' \\ \sqrt{\epsilon}y_2' \\ x_2' \end{pmatrix} = \begin{pmatrix} y_2 \\ x_2 \\ (T^2 D^{-1}J^{-1}M^{-1}\Phi_q^T)\lambda + \left(T^2 D^{-1}J^{-1}M^{-1}(u-h) - TJ^{-1}\dot{J}\begin{pmatrix} \sqrt{\epsilon}y_2 \\ x_2 \end{pmatrix} \right) \end{pmatrix}, \quad (21)$$

where $'$ denotes the differentiation with respect to $\bar{t}$, $D = \begin{pmatrix} L \cdot I_{k \times k} & 0 \\ 0 & D_2 \end{pmatrix}$, and $\lambda_i = f_i(-\epsilon L y_{1,i}) + g_i(-\epsilon L y_{1,i}, -\sqrt{\epsilon}y_{2,i}L/T)$. Here we use the notation $y_{i,j}$ to refer to the jth component of the vector y_i. $\mathbf{x}(\bar{t})$ and $\mathbf{y}(\bar{t})$ represent the dimensionless slow and fast trajectories, respectively.

The differential equations for the fast variables are given by

$$\sqrt{\epsilon}\mathbf{y}' = \begin{pmatrix} y_2 \\ A(\mathbf{x},\mathbf{y},\epsilon)\bar{\lambda}(\mathbf{y},\epsilon) + B(\mathbf{x},\mathbf{y},\epsilon) \end{pmatrix} \quad (22)$$

with

$$\bar{\lambda}(\mathbf{y},\epsilon) = \begin{pmatrix} \bar{\lambda}_N(\mathbf{y},\epsilon) \\ \bar{\lambda}_{TR}(\mathbf{y},\epsilon) \end{pmatrix} = \frac{T^2}{D_M L}\begin{pmatrix} \lambda_N \\ \lambda_{TR} \end{pmatrix}, \quad \bar{\lambda}_N(\mathbf{y},\epsilon) \geq 0,$$

$$A(\mathbf{x},\mathbf{y},\epsilon) = D_M L (D^{-1}J^{-1}M^{-1}\Phi_q^T)_{kk},$$

$$B(\mathbf{x},\mathbf{y},\epsilon) = (T^2 D^{-1}J^{-1}M^{-1})_{kn}(u-h) - (TJ^{-1}\dot{J})_{kn}\begin{pmatrix} \sqrt{\epsilon}y_2 \\ x_2 \end{pmatrix},$$

where D_M is the characteristic mass. Here, $(\cdot)_{\alpha\beta}$ refers to the submatrix in (.) consisting of the first α rows and the first β columns. As ϵ goes to zero, Eq. (22) degenerates into the following algebraic equations:

$$\begin{pmatrix} y_2 \\ A(\mathbf{x},\mathbf{y},0)\bar{\lambda}(\mathbf{y},0) + B(\mathbf{x},\mathbf{y},0) \end{pmatrix} = 0_{2k \times 1}. \quad (23)$$

We say that the singular perturbation model (21) is in standard form if and only if the above algebraic equations have at least one isolated real root for $\mathbf{y}$ in terms of $\mathbf{x}$. We will proceed with the stability analysis with the assumption that Eq. (23) has at least one feasible solution $\mathbf{y}_0(\mathbf{x})$. We now look at the solution to Eq. (21) with $\mathbf{y} = \mathbf{y}_0(\mathbf{x})$ and $\epsilon = 0$. This solution, denoted by $\mathbf{x}_0(\bar{t})$, is the solution of the reduced rigid-body system.

Assume that $\mathbf{x}_0(\bar{t})$ is defined for $\bar{t} \in [0, \bar{t}_1]$. At an arbitrary time instance $\bar{t}_0 \in [0, \bar{t}_1]$, the boundary layer system of (22) can be introduced through a "stretch" of the time scale, $\tau = \bar{t} - \bar{t}_0/\sqrt{\epsilon}$. In the stretched time scale τ, the variables $\bar{t}$ and $\mathbf{x}(\bar{t}, \epsilon)$ are slowly varying. Since $\bar{t}_0$ is allowed to take any value in $[0, \bar{t}_1]$, the boundary layer system of (22) can be written with τ as the independent variable:

$$\mathbf{y}' = \begin{pmatrix} y_2 \\ A(\mathbf{x}_0,\mathbf{y},0)\bar{\lambda}(\mathbf{y},0) + B(\mathbf{x}_0,\mathbf{y},0) \end{pmatrix} \quad (24)$$

where $'$ now denotes differentiation with respect to τ. Let

$$\begin{pmatrix} z \\ z' \end{pmatrix} = \mathbf{y} - \mathbf{y}_0(\mathbf{x}_0).$$

Perform a linearization of the boundary layer model (24) around the equilibrium solution $\mathbf{y}_0(\mathbf{x}_0)$. We obtain the homogeneous boundary layer dynamics of the form

$$z'' + Pz' + Qz = 0_{k \times 1}, \quad (25)$$

with

$$P = -\frac{\partial(A(\mathbf{x}_0,\mathbf{y},0)\bar{\lambda}(\mathbf{y},0) + B(\mathbf{x}_0,\mathbf{y},0))}{\partial y_2}\bigg|_{\mathbf{y}=\mathbf{y}_0(\mathbf{x}_0)},$$

$$Q = -\frac{\partial(A(\mathbf{x}_0,\mathbf{y},0)\bar{\lambda}(\mathbf{y},0) + B(\mathbf{x}_0,\mathbf{y},0))}{\partial y_1}\bigg|_{\mathbf{y}=\mathbf{y}_0(\mathbf{x}_0)}.$$

The response of the above system equation, $z(\tau)$, is the transient that describes the dynamics associated with the compliance at the contact points. The stability of the system implies the convergence of the compliant contact model solution $\mathbf{x}(\bar{t}, \epsilon)$ to the rigid-body model solution $\mathbf{x}_0(\bar{t})$. We can directly apply Tikhonov's theorem [19] to get the following result:

THEOREM 4.1 *Consider the system described by (21) and let $\mathbf{y}_0(\mathbf{x})$ be an isolated solution of (23). If the following three conditions are satisfied by $(\mathbf{x}(\bar{t}), \mathbf{y}(\bar{t}), \epsilon)$ for all $\bar{t} \in [0, \bar{t}_1]$ and $\epsilon \in [0, \epsilon_0]$: (a) the terms on the right-hand side of (21) and their first partial derivatives with respect to $(\mathbf{x}, \mathbf{y}, \epsilon)$ are bounded and continuous; (b) the origin of the boundary layer system (25) is exponentially stable; and (c) $\mathbf{y}_0(\mathbf{x})$ has continuous first partial derivatives with respect to its arguments, then the following are true:*

- *The reduced rigid-body model, obtained from (21) by substitution of $\mathbf{y} = \mathbf{y}_0(\mathbf{x})$ and $\epsilon = 0$, has a unique bounded solution, $\mathbf{x}_0(\bar{t})$, for all $\bar{t} \in [\bar{t}_0, \bar{t}_1]$, where $\bar{t}_0 \in [0, \bar{t}_1]$.*
- *There exist positive constants δ_0 and ϵ_0 such that for the initial conditions $\mathbf{x}(\bar{t}_0, \epsilon)$ and $\mathbf{y}(\bar{t}_0, \epsilon)$ satisfying $\|\mathbf{y}(\bar{t}_0, \epsilon) - \mathbf{y}_0(\mathbf{x}(\bar{t}_0, 0))\| < \delta_0$ and $0 < \epsilon < \epsilon_0$, the singular perturbation problem has a unique solution $\mathbf{x}(\bar{t}, \epsilon)$ and $\mathbf{y}(\bar{t}, \epsilon)$ on the interval $[\bar{t}_0, \bar{t}_1]$ and*

$$\mathbf{x}(\bar{t}, \epsilon) - \mathbf{x}_0(\bar{t}) = O(\sqrt{\epsilon}), \quad \mathbf{y}(\bar{t}, \epsilon) - \mathbf{y}_0(\bar{t}) = O(\sqrt{\epsilon}).$$

Proof: The proof of this theorem follows directly from Tikhonov's theorem, and is a direct application of Theorem 9.1 in [19].

Remark 4.1

- The stability of the boundary layer system is determined by the matrices P and Q, or specifically, the eigenvalues of $\begin{pmatrix} 0_{k \times k} & I_{k \times k} \\ -Q & -P \end{pmatrix}$.

- Other than the general constitutive model described by Eqs. (7) and (8), no specific compliant contact models are introduced in the discussion, therefore the stability results will not change when different compliant models are employed.

It is worth noting that the requirements on the continuity of the first partial derivatives in Theorem 4.1 are not satisfied whenever there are transitions from rolling to sliding or sliding to rolling because of the nonsmooth nature of Coulomb's law. In the next section, we will apply Theorem 4.1 to planar mechanical systems with one contact and discuss the cases of sliding and rolling separately.

5 Planar Mechanical Systems With One Contact

Consider the planar rigid body depicted in Fig. 2 in contact with a horizontal surface, where L is the distance from the contact point to the center of mass (CM). The rigid body has mass m and centroidal moment of inertia I. $q = (y \ x \ \theta)^T$ represent the generalized coordinates for the rigid body which are the position of the CM and the angular orientation. (F_x, F_y) are the external forces acting on the body and F_θ is the external moment about the CM. μ is the coefficient of friction between the rigid body and surface. The equations of motion for the system with one contact are given by Eq. (1) with

$$q = \begin{pmatrix} y \\ x \\ \theta \end{pmatrix}, \quad M = \begin{pmatrix} m & 0 & 0 \\ 0 & m & 0 \\ 0 & 0 & I \end{pmatrix}, \quad u = \begin{pmatrix} F_y \\ F_x \\ F_\theta \end{pmatrix}, \quad \text{and} \quad h = 0_{3 \times 1}.$$

$$(26)$$

For sliding contact:

$$\Phi_q^T = (1 \quad \mu_s \quad \mu_s L \sin \theta - L \cos \theta)^T, \quad \lambda = \lambda_N = \lambda_{NS}, \quad (27)$$

and for rolling contact:

$$\Phi_q^T = \begin{pmatrix} 1 & 0 \\ 0 & 1 \\ -L \cos \theta & L \sin \theta \end{pmatrix}, \quad \lambda = \begin{pmatrix} \lambda_{NR} \\ \lambda_{TR} \end{pmatrix}, \quad (28)$$

where $\mu_s = -\mu \, \text{sign}(\Phi_T)$.

5.1 Sliding Contact. For the sliding case, the rigid-body dynamics can be modeled as a LCP of the form

$$\Phi_N = A \lambda_N + B \qquad (29)$$

where

$$\Phi_N \geq 0, \quad \lambda_N \geq 0, \quad \text{and} \quad \Phi_N \lambda_N = 0,$$
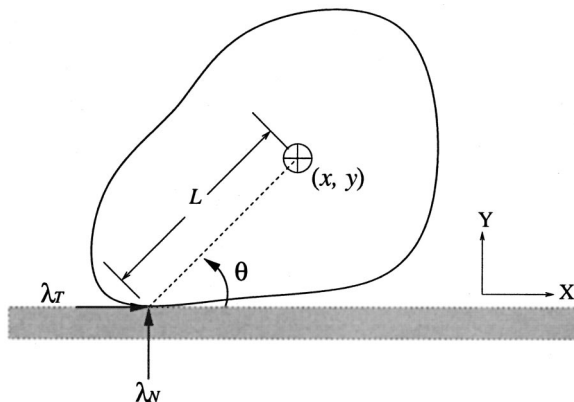
Fig. 2 Planar rigid body in contact with a rough surface

$$A = \frac{1}{m} + \frac{L^2 \cos \theta}{I} (\cos \theta - \mu_s \sin \theta),$$

$$B = L \dot\theta^2 \sin \theta + \frac{F_y}{m} - \frac{L \cos \theta F_\theta}{I}.$$

Note with $\mu_s = 0$, $A > 0$ and therefore A is a 1×1 P matrix, which guarantees a unique solution. If $B \geq 0$ we are guaranteed of the existence of a solution regardless of whether or not A is a P matrix.

We now proceed with the singular perturbation approach to the problem. A transformation to a system of fast and slow variables can be accomplished by making the change of variables as

$$q_1 = y, \quad q_2 = \begin{pmatrix} x \\ \theta \end{pmatrix}, \quad p_1 = \Phi_N, \quad \text{and} \quad p_2 = q_2.$$

Use (19) and (20) to nondimensionalize the state variables with

$$D_1 = d_1, \quad D_2 = \begin{pmatrix} L & 0 \\ 0 & 1 \end{pmatrix}, \quad \text{and} \quad \epsilon = \frac{d_1}{L}.$$

Let the characteristic mass $D_M = m$, the mass of the rigid body. The standard singular perturbation form of the planar rigid-body system with one sliding contact is given by

$$\begin{cases} \sqrt{\epsilon} \mathbf{y}' = \begin{pmatrix} y_2 \\ A(\mathbf{x}) \bar\lambda_N(\mathbf{y}, \epsilon) + B(\mathbf{x}) \end{pmatrix} \\ \mathbf{x}' = \begin{pmatrix} x_2 \\ \mu_s \bar\lambda_N(\mathbf{y}, \epsilon) + \bar F_x \\ \dfrac{mL^2}{I} (\mu_s \sin x_{1,2} - \cos x_{1,2}) \bar\lambda_N(\mathbf{y}, \epsilon) + \bar F_\theta \end{pmatrix} \end{cases}$$

$$(30)$$

where

$$\bar\lambda_N(\mathbf{y}, \epsilon) = \frac{f_N(-\epsilon L y_1) + g_N\left(-\epsilon L y_1, -\dfrac{\epsilon L}{T} \mathbf{y}_2\right)}{\dfrac{mL}{T^2}} \geq 0,$$

$$A(\mathbf{x}) = 1 + \frac{mL^2}{I} \cos x_{1,2} (\cos x_{1,2} - \mu_s \sin x_{1,2}),$$

$$(31)$$

$$B(\mathbf{x}) = x_{2,2}^2 \sin x_{1,2} - \bar F_\theta \cos x_{1,2} + \bar F_y,$$

$$\bar F_x = \frac{F_x}{\dfrac{mL}{T^2}}, \quad \bar F_y = \frac{F_y}{\dfrac{mL}{T^2}}, \quad \text{and} \quad \bar F_\theta = \frac{F_\theta}{\dfrac{I}{T^2}}.$$

Note that the symbol $x_{i,j}$ refers to the jth component of the vector x_i. By following through the same derivations given by Eqs. (21)–(25) in Section 4, the linearized boundary layer model of (30) can be obtained as

$$z'' - A(\mathbf{x}_0) \left(\frac{\partial \bar\lambda_N(\mathbf{y}, 0)}{\partial y_2} \right) \Bigg|_{\mathbf{y} = \mathbf{y}_0(\mathbf{x}_0)} z' - A(\mathbf{x}_0)$$

$$\times \left(\frac{\partial \bar\lambda_N(\mathbf{y}, 0)}{\partial y_1} \right) \Bigg|_{\mathbf{y} = \mathbf{y}_0(\mathbf{x}_0)} z = 0, \qquad (32)$$

where $\mathbf{y}_0(\mathbf{x})$ is a solution of the algebraic equations obtained by setting $\epsilon = 0$ in (30), and $\mathbf{x}_0(\bar t)$ is the solution of the reduced system of (30) corresponding to $\mathbf{y}_0$.

In a general viscoelastic model, it is reasonable to assume that $\bar\lambda_N$ is a monotonically decreasing function with respect to y_1 and y_2. With this assumption, if $A(\mathbf{x}_0, 0)$ is positive, the boundary layer system (25) is stable, and the stability of the solution for the

Table 1 LCP and stability results for one sliding contact (*C* =contact, *NC*=no contact, *NS*=no solution, *RB* =rigid-body model, *CC*=compliant contact model;* indicates that the stability result comes from the fact that the noncontact solutions (free falling) are always stable)

Conditions		Solutions	Stability	Preferred Model
$A>0$	$B\geqslant0$	NC	stable*	RB
$A>0$	$B<0$	C	stable	RB
$A=0$	$B>0$	NC	stable*	RB
$A=0$	$B=0$	∞ solns.	-	CC
$A=0$	$B<0$	NS	N/A	CC
$A<0$	$B\geqslant0$	C	unstable	discard
		NC	stable*	RB
$A<0$	$B<0$	NS	N/A	CC

singular perturbation problem (21) is guaranteed if all other conditions in Theorem 4.1 are satisfied. In a single point sliding contact problem, the rigid-body LCP formulation (29) has a unique solution if and only if $A(\mathbf{x}_0,0)$ is positive. The above conclusion can be summarized into the following theorem.

THEOREM 5.1 *For a planar rigid body with a single sliding contact described by (1) and (27), the solution obtained from the compliant contact model converges to that obtained from the rigid-body model if and only if there exists a unique solution for the rigid body LCP formulation (29). This result is independent of the compliant contact models as long as the monotonicity condition, $-\partial\bar{\lambda}_N(\mathbf{y}(t),0)/\partial y_{1,2}>0$, is satisfied.*

As examples, we show that the stability results are the same for both the Kelvin-Voigt and the Hunt-Crossley models. From Eq. (10) and the expression in (31), the dimensionless normal contact force for Kelvin-Voigt model can be written as

$$\bar{\lambda}_N(\mathbf{y},\epsilon)=\bar{\lambda}_N(\mathbf{y})=-\bar{K}y_1-\bar{C}y_2. \quad (33)$$

where the nondimensional stiffness and the damping are defined as

$$\bar{K}=\frac{K}{\dfrac{1}{\epsilon L}\dfrac{mL}{T^2}}>0 \quad \text{and} \quad \bar{C}=\frac{C}{\dfrac{1}{\sqrt{\epsilon L/T}}\dfrac{mL}{T^2}}>0. \quad (34)$$

The boundary layer system is obtained as

$$z''+A(\mathbf{x}_0)\bar{C}z'+A(\mathbf{x}_0)\bar{K}z=0. \quad (35)$$

For Hunt-Crossley model, the normal contact force can be expressed as

$$\bar{\lambda}_N(\mathbf{y},\epsilon)=\bar{\lambda}_N(\mathbf{y})=\bar{K}(-y_1)^\beta-\bar{\alpha}\bar{K}(-y_1)^\beta y_2, \quad (36)$$

where

$$\bar{K}=\frac{K}{\dfrac{1}{(\epsilon L)^\beta}\dfrac{mL}{T^2}}>0 \quad \text{and} \quad \bar{\alpha}=\frac{3}{2}\frac{\alpha}{\dfrac{1}{\sqrt{\epsilon L/T}}}>0. \quad (37)$$

The linearized boundary layer system for Hunt-Crossley model is given by

$$z''+A(\mathbf{x}_0)\bar{\alpha}\bar{K}(-y_1)^\beta|_{\mathbf{y}=\mathbf{y}_0(\mathbf{x}_0)}z'+A(\mathbf{x}_0)\beta\bar{K}(-y_1)^{\beta-1}|_{\mathbf{y}=\mathbf{y}_0(\mathbf{x}_0)}z$$

$$=0. \quad (38)$$

Since $y_1\leqslant0$ for any active constraint, it is clear that the stability of the boundary layer dynamics, described by either (35) or (38), depends entirely on the value of $A(\mathbf{x}_0)$. Thus, independent of the choice of contact model, $A(\mathbf{x}_0)$ may used to test contact force stability in those situations where the LCP tells us that the contact is maintained. A summary of the results is given in Table

1. For the contact maintaining solutions, the result of the singular perturbation analysis states that stability only occurs where the quantity *A* in the LCP formulation is positive (*P* matrix). If the LCP reports an unique solution, we use the rigid-body model to simulate the dynamic motion. For the case when the LCP has two solutions ($A<0,B\geqslant0$), we can still use the rigid-body model since the stability analysis shows a unique stable solution.

5.2 Rolling Contact. The rigid-body dynamics can once again be formulated as an LCP with the help of surplus and slack variables ([7]). The singular perturbation analysis proceeds in exactly the same way as in the previous section. The following is a partition of the generalized coordinates for the rolling case:

$$q_1=\begin{pmatrix}y\\x\end{pmatrix}, \quad q_2=\theta, \quad p_1=\begin{pmatrix}\Phi_N\\\Phi_T\end{pmatrix}, \quad \text{and} \quad p_2=q_2.$$

The linearized boundary layer model for this case is given by

$$z''-A(\mathbf{x}_0)\left(\frac{\partial\bar{\lambda}(\mathbf{y},0)}{\partial y_2}\right)\bigg|_{\mathbf{y}=\mathbf{y}_0(\mathbf{x}_0)}z'-A(\mathbf{x}_0)\left(\frac{\partial\bar{\lambda}(\mathbf{y},0)}{\partial y_1}\right)\bigg|_{\mathbf{y}=\mathbf{y}_0(\mathbf{x}_0)}z$$

$$=0_{2\times1}, \quad (39)$$

where

$$\bar{\lambda}=(\bar{\lambda}_{NR}^T \ \bar{\lambda}_{TR}^T)^T,$$

$$A(\mathbf{x})=\begin{pmatrix}1+\dfrac{mL^2}{I}\cos^2x_1 & -\dfrac{mL^2}{I}\sin x_1\cos x_1\\[2mm] -\dfrac{mL^2}{I}\sin x_1\cos x_1 & 1+\dfrac{mL^2}{I}\sin^2x_1\end{pmatrix},$$

$$B(\mathbf{x})=\begin{pmatrix}\bar{F}_y-\bar{F}_\theta\cos x_1+x_2^2\sin x_1\\\bar{F}_x+\bar{F}_\theta\sin x_1+x_2^2\cos x_1\end{pmatrix}. \quad (40)$$

In the above system, $A(\mathbf{x}_0)$ is symmetric, and its eigenvalues are given by $a_1=1$, $a_2=1+mL^2/I$ which are positive real numbers. Also if $\bar{\lambda}$ is a monotonically decreasing function with respect to **y**, both $-\partial\bar{\lambda}(\mathbf{y}_0,0)/\partial y_1$ and $-\partial\bar{\lambda}(\mathbf{y}_0,0)/\partial y_2$ are diagonal matrices with positive entries. In this situation, the stability of the boundary layer system (39) follows from the Routh-Hurwitz criterion. The reason is that for rolling constraints, the contact model corresponds instantaneously to a frictionless (no dissipation) complaint pin joint. Viewed in this context, the contact forces correspond to the joint constraint forces. It is not surprising that, in the rigid-body limit, these forces are always stable. In contrast, the singular perturbation analysis of sliding included the dependence of tangential friction force on normal force. This dependence produced the potential for instability during sliding. Since the LCP and singular perturbation analyses for sliding both included this dependence, it was possible in Theorem 5.1 to relate the LCP existence and uniqueness results to the singular perturbation stability result.

There are three possible solutions for the LCP formulation of a system with a rolling contact: (a) breaking contact, (b) continued rolling, and (c) transition to sliding. The conditions of Theorem 4.1 for use of the rigid-body model include continuity and differentiability of the tangential contact forces. These conditions are not met during (a) or (c) because the contact forces need only be C^0 continuous at a transition. Therefore, we cannot derive a result similar to Theorem 5.1 for rolling contacts. It is possible, however, to state the more conservative result:

THEOREM 5.2 *For a planar rigid-body with a single rolling contact described by (1) and (28), the solution obtained from the compliant contact model converges to that obtained from the rigid-body model whenever the LCP formulation yields a unique*

solution corresponding to continued rolling. This result is independent of the compliant contact models as long as the monotonicity condition of λ is satisfied.

5.3 Extensions. In the treatment thus far, we considered the dynamics of a single rigid body in which the unilateral constraints were due to one contact (sliding or rolling) with a second fixed rigid body. When we consider multiple planar rigid bodies with bilateral constraints, but only one contact, a similar result can be derived. In such a case, the dynamics formulations in the Cartesian space and the constraints can still be described by (1) and (27), (28), if the operational space inertia matrix, M, exists. The only differences are that the inertia matrix, if it exists, is no longer diagonal but symmetric and still positive definite, and $h(q,\dot{q})$ is no longer zero. But these differences will not affect the properties of the A matrix in the boundary layer systems (32) and (39). Consequently, the basic ideas developed in this section are still valid, and the main results are applicable to any mechanical system in which the unilateral constraints are due to a single contact.

6 Results From Experiments and Simulations

In this section, we compare the results of numerical simulations with experimental observations. In the experiments, an aluminum rod with spherical ends is released from rest, while contacting a flat, rough, fixed surface, with different initial positions. We used the OPTOTRAK-3020 (Northern Digital, Inc.), a noncontact three-dimensional motion measurement system with an accuracy better than 0.1 mm in each coordinate direction and a tracking rate can be as high as 1000Hz. The experimental setup is shown in Fig. 3.

The numerical simulation is based on the dynamics given by Eqs. (1) and (27). The length and diameter of the tested rod are 0.468 m and 0.00948 m, respectively. The mass is 0.088 kg. The compliant model used in the simulations is the Hunt-Crossley model expressed by Eqs. (36)–(37). The only unknown parameter in the equations is the coefficient of friction. The coefficient of friction for the simulation is chosen to be the value that best approximates experimentally observed trajectories in a least-squares sense.

6.1 Case 1: The LCP has a Unique Solution. We first consider an experiment in which our rigid-body LCP predicts a unique solution throughout the duration of the experiment. The initial conditions of the rod are $\theta = 42.3$ deg, $\dot{\theta} = 0$, and $\dot{x} = \dot{y} = 0$. The external force are $F_x = 0$, $F_y = -$mg, and $M_z = 0$. The related parameters used in Hunt-Crossley model are $\bar{K} = 1$, $\bar{\alpha} = 1$, and $\beta = 2$. The trajectory corresponds to a condition of sliding where the contact point slides to the left. The sliding velocity decreases, and

at approximately 0.205 sec, the sliding velocity changes direction so that the contact point slides to the right. In Fig. 4, we show the experimentally observed trajectory and the simulation results for (a) the trajectory of contact point, (b) the normal contact force, and (c) the tangential contact force. The simulation results are provided for the rigid-body LCP solution and for the compliant contact model for a range of ϵ values. The coefficient of friction used in the simulation is $\mu = 0.27$.

The first thing to note is that there is a close agreement between the experimental trajectory and the rigid-body LCP solution with the same initial condition as expected. The second issue to focus on is the set of results from the simulation of the compliant contact model. Even though the initial condition for the compliant contact model solution is different from the equilibrium solution, it quickly converges to the equilibrium solution. The convergence in an absolute time scale is faster as ϵ becomes smaller. This is also evident at the transition from reverse to forward sliding, which includes a very brief period of rolling. The discontinuity of the rigid-body dynamic model with Coulomb friction is seen in the contact force variation in Figs. 4(*b*) and 4(*c*). However, the compliant contact model yields a continuous solution that can be made to approach the solution of the LCP model arbitrarily closely by letting ϵ assume very small values.

6.2 Case 2: The LCP has Two Solutions. In Section 5 we showed that, in cases when the LCP formulation for sliding contact has two solutions, the model of the boundary layer system (32) predicts that the contact maintaining solution is unstable. In such cases, at any instant, the LCP predicts two possible outcomes. While it is possible to simulate either outcome using the compliant contact model, a simulation based on the rigid-body model involves making a choice at each such point.

An ideal uniform rod with $L = 1$ m and $m = 1$ kg is used in the simulation. The initial condition of the rod are $\theta = 70$ deg, $\dot{\theta} = 0$, and $\dot{x} = \dot{y} = 0$. The external forces are $F_x = 0$, $F_y = -$mg, and $M_z = -1$ Nm. The coefficient of friction is $\mu = 1$. The compliant contact model used in the simulation is the Hunt-Crossley model with the same parameters as in Case 1. Because this case can only be achieved at carefully chosen values of external forces or initial velocities, we were unable to reproduce this case experimentally.

In Fig. 5, we show the results of the rigid-body solution assuming that (a) the contact breaks at $t = 0$—the first solution; and (b) the contact is maintained at $t = 0$—the second solution, and at future time instants as well. The main point to be observed in Fig. 5 is the performance of the compliant contact model. As shown in Fig. 5(*b*), even when started from the condition of maintaining contact, the solution for the compliant contact model exponentially converges to the stable solution of no contact. The rate of
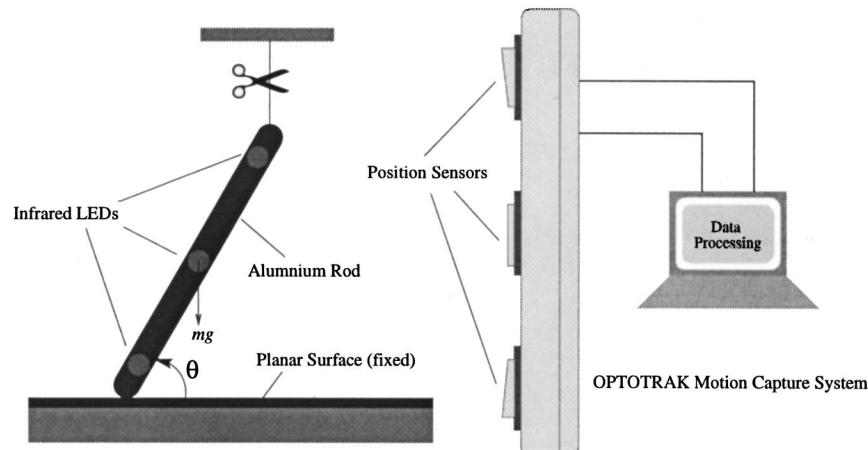
Fig. 3 The experimental setup
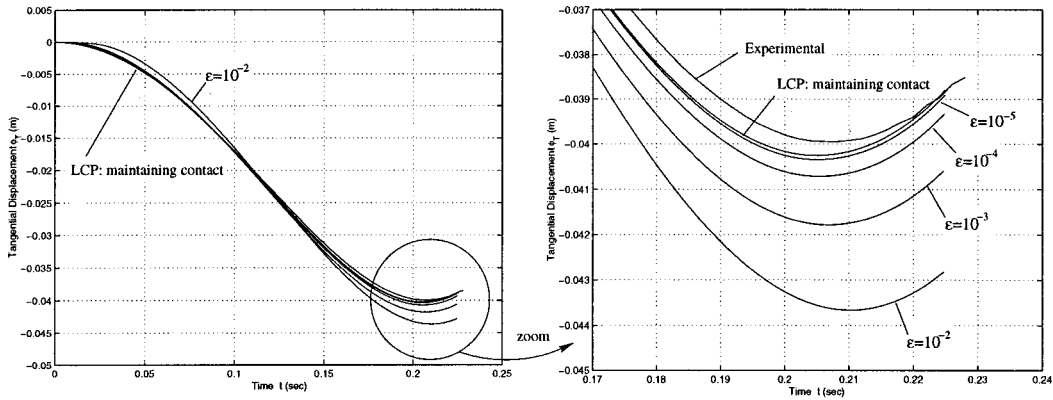
(a) Tangential displacement of the rod at the contact point
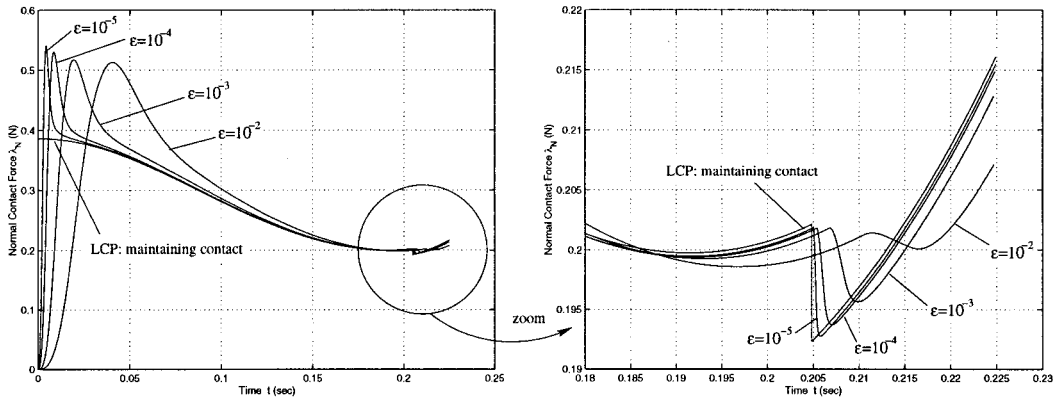
(b) History of the normal contact force
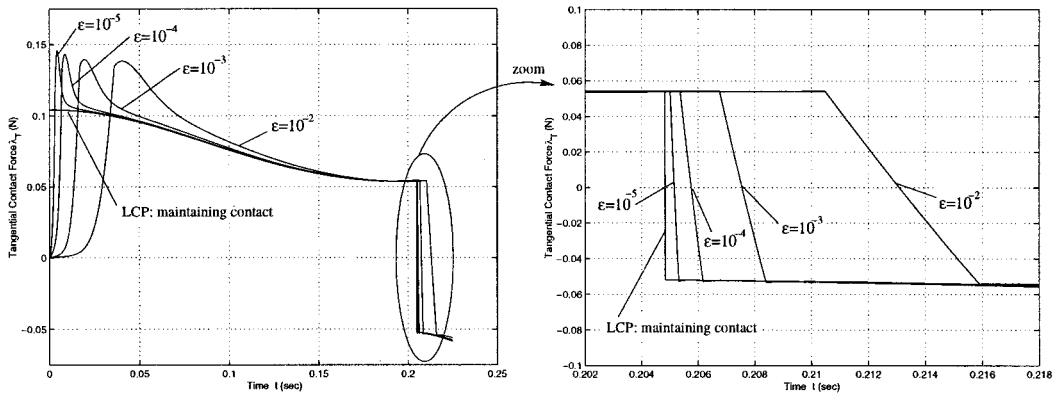
(c) History of the tangential contact force

Fig. 4   Case 1: The LCP has a unique solution and the compliant contact model solution converges to the rigid-body model solution as the perturbation parameter ϵ goes to 0

convergence increases with decreasing ϵ. In contrast, at $t = 0.163$ sec, the rigid-body solution corresponding to maintaining contact reaches a state where the LCP has a unique solution corresponding to contact separation. This can be seen in Fig. 5(b) as the discontinuous drop in normal contact force. The fact that the compliant model solution converges to the stable rigid-body model solution indicates that in cases when LCP has two solu-

tions, one stable and one unstable, we can always choose the stable solution and use the rigid body model to continue the simulation.

7   Friction Models

There are many types of friction phenomena and equations to model them. Coulomb friction is one of the simplest and in many
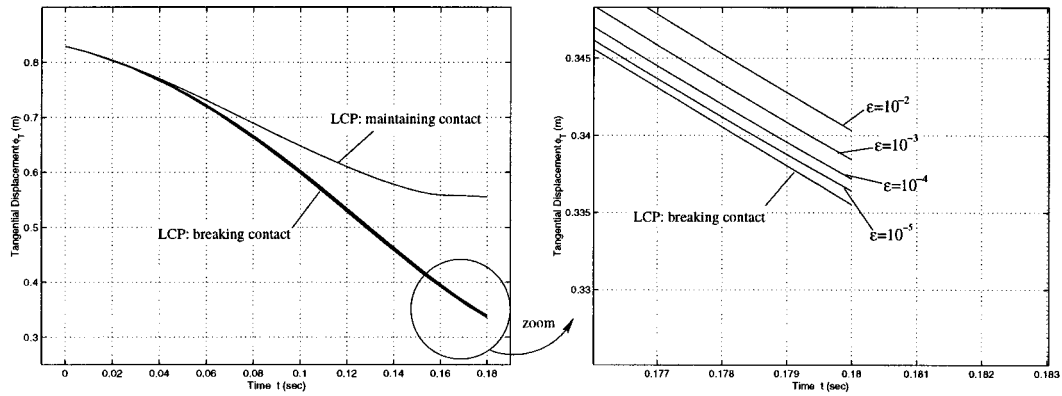
(a) Tangential displacement of the rod at the contact point
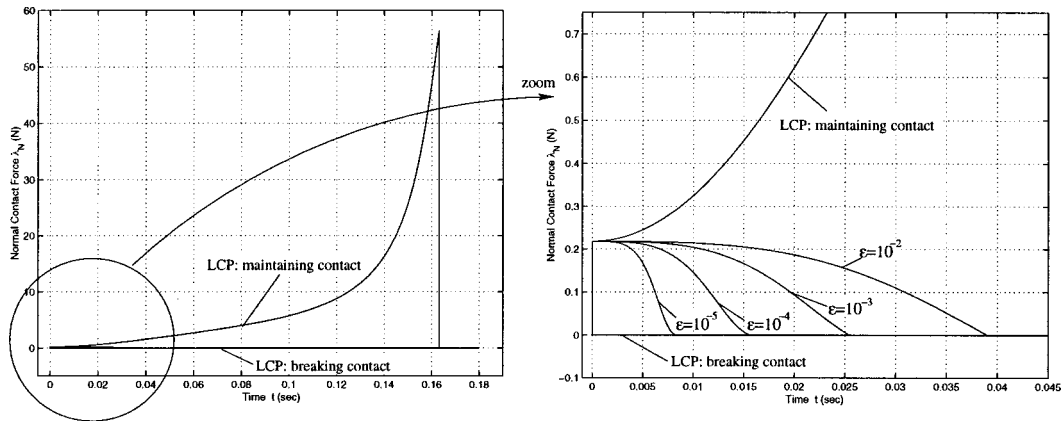
(b) History of the normal contact force

Fig. 5   Case 2: The LCP has two solutions, maintaining contact (unstable) and separation (stable). If the compliant model solution is started with the unstable maintaining contact solution, it quickly converges to the separation solution (stable).

situations can adequately predict the system's behavior. Nevertheless, its mathematical properties complicate dynamic simulation for both rigid-body and compliant contact models. The difficulties caused by Coulomb's friction model in rigid-body dynamic simulation are due to the following issues: (1) the friction force is not smooth during rolling-sliding transitions; and (2) during rolling, the friction force cannot be directly determined from the state variables. When solving the forward dynamic problem, these two issues can either increase the complexity of the system or cause analytical difficulties. Specifically the rolling and sliding constraints need to be handled differently in the rigid-body formulations ([7]). This is also the main reason that our stability results in Section 4 are not applicable to transitions from rolling to sliding. Furthermore, cases arise in which a unique solution to the forward dynamics problem does not exist.

Since these difficulties are due to the Coulomb model, it is possible to overcome them by substituting a model with the requisite mathematical properties. In fact, nonclassical friction laws which are nonlinear and nonlocal have been found to be superior to pointwise Coulomb models from both a phenomenological and a computational viewpoint ([22]). A few of these models were developed specifically for rigid-body dynamics. For example, a discontinuous model that extends the Coulomb's stiction zone from zero velocity to a small neighborhood of zero velocity is

suggested in ([23]). Many others ([12]), including Dahl's model and the bristle model, can be considered to be extensions of the compliant contact model.

Our interest is in the simplest friction law that approximates Coulomb friction and is a continuously differentiable function of the system states. Such a model would allow us to formulate the dynamics using either rigid-body models or compliant contact
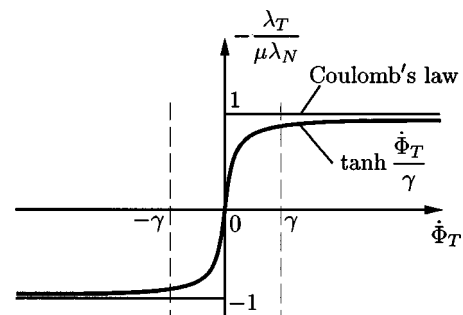
Fig. 6   A smooth, nonlinear friction law with two parameters γ, a characteristic speed, and μ, the coefficient of friction
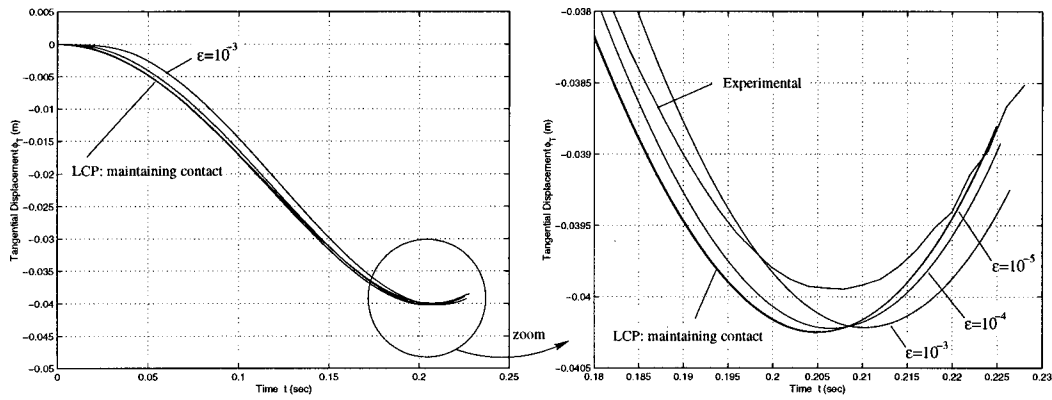
(a) Tangential displacement of the rod at the contact point
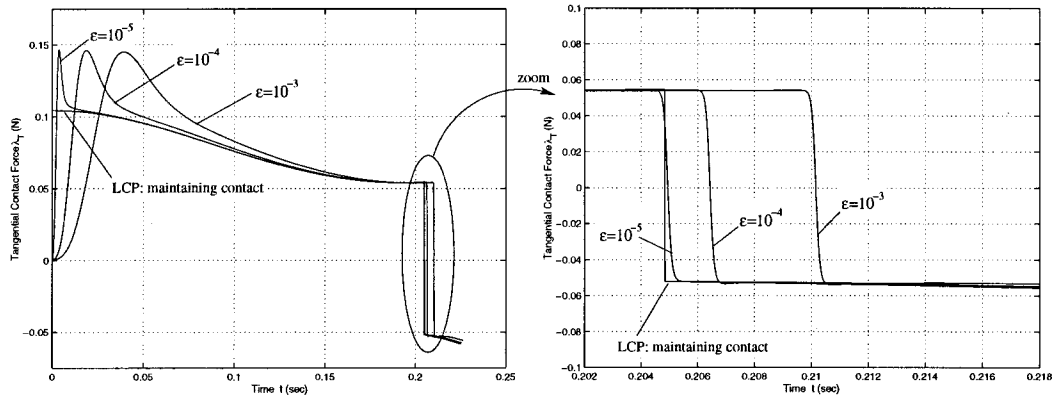
(b) History of the tangential constraint force

Fig. 7 Results with the smooth nonlinear friction law ($\gamma = 10^{-3}$). The transition from reverse sliding to rolling to forward sliding at $t = 0.205$ sec is characterized by a smooth variation of contact forces.

models while improving the performance of both. A friction law with these properties is shown in Fig. 6. It has a one-to-one correspondence between the friction force λ_T and the relative tangential velocity $\dot{\Phi}_T$. The small parameter γ defines the extent of the "rolling" regime: $\dot{\Phi}_T \in [-\gamma, \gamma]$. By letting γ tend to zero, we can obtain an arbitrarily close approximation to Coulomb's law, albeit with some sliding in the "rolling" regime. Using this friction law with the rigid-body dynamic model expressed in Eqs. (1)–(2), we no longer need to differentiate between rolling and sliding contacts. Instead, the Jacobian matrix (Φ_q) in Eq. (3) always takes the form

$$\Phi_q^T = \left[\Phi_{N_q}^T - \Phi_{T_q}^T \operatorname{diag}\left(\mu \tanh\left(\frac{\dot{\Phi}_T}{\gamma} \right) \right) \right]. \tag{41}$$

This gives rise to a unified LCP formulation that works for both rolling and sliding constraints. The smooth friction law can also improve numerical performance of the compliant contact model, since we no longer need the deformation state vector, δ_T, to compute the tangential force which is uniquely defined by the normal contact force and the relative velocity.

$$\lambda_{T,i} = -\mu \tanh\left(\frac{\dot{\Phi}_{T,i}}{\gamma} \right) \lambda_{N,i} \tag{42}$$

As is the case with rigid-body dynamics and Coulomb's law, the LCP formulation with the smooth friction law will have situ-

ations with no solution or multiple solutions. And, as before, the compliant contact model given by Eqs. (12) and (42) resolves the difficulties with uniqueness and existence. Since the stability analysis in Section 4 can be easily applied to this new frictional model without worrying about transitions between rolling and sliding contacts, Theorem 5.1 can be directly extended to any planar mechanical system with a single rolling or sliding contact. Because the rolling constraint is now replaced by "microsliding" with the tangential contact velocity smaller than γ, the proof follows exactly the same lines of the proof in Section 5.1.

To illustrate the effect of the smooth friction law, we consider the same situation shown in Fig. 4 (Case 1 in Section 6). Recall the transition from reverse sliding to rolling to forward sliding in Fig. 4 at $t = 0.205$ sec. Figure 7 shows the results of the simulation with the smooth friction law with the same initial conditions. The rigid-body model predicts discontinuities in the contact forces. However, the compliant contact predicts a smooth transition from sliding to sticking (relative velocity less than the threshold γ) to sliding in the opposite direction.

The main disadvantage of the nonlinear friction law is due to the fact a static friction force can only be maintained through "creep" in the tangential direction. While the "creep" rate is less than γ, and γ can be set to a very small value, it is not a very attractive solution because it has the adverse effect of making the system of ODEs stiff. There is a natural tradeoff that must be considered in selecting the parameter γ.

8   Concluding Remarks

When rigid-body models are used in conjunction with Coulomb friction for dynamic simulation of systems with frictional contacts, there may be situations in which there are no solutions or multiple solutions for the contact forces and the accelerations. In this paper, we describe a contact model that models the small compliance in the normal and tangential directions. We show that this compliant contact model, when used with the rigid-body dynamic equations of motion, always yields a unique solution for the accelerations and the forces. While this model is superior to the traditional rigid-body model in terms of accuracy and robustness, it is also more complex and requires a larger number of parameters. Therefore, it is appealing to use rigid-body models, whenever concerns of uniqueness and existence do not arise.

The main contribution of this paper is the use of singular perturbation theory to establish conditions under which solutions from the rigid-body model are stable, or in other words, conditions in which the compliant contact model solution converges exponentially to the rigid-body model solution. In situations when rigid-body LCP analysis reveals multiple solutions, stability analysis can resolve the ambiguity. We can simply discard the unstable solutions and retain the stable one. The stability analysis shows when it is essential to pursue the more sophisticated compliant contact model, and when it is satisfactory to neglect the fast dynamics. The basic issues are illustrated with the help of a simple example with one contact that may be rolling, sliding, or separating. The case of rolling contacts poses an additional difficulty because of the fact the tangential forces obtained by Coulomb-like frictional laws, even when used with compliant contact models, are not smooth functions of the state. The second main contribution of the paper is the result that a smooth nonlinear friction law, inspired by Oden and Pires' nonlinear friction law ([22]), overcomes this difficulty. We show that in the case of planar mechanical systems with one contact, there are at most two solutions, and there is only one stable solution.

The basic ideas of this paper are applicable to any situation with frictional contacts. However, in order for the rigid-body model, and therefore the perturbation analysis to be applicable, we are limited to planar problems with three or less independent constraints and spatial problems with six or less independent constraints. Note the compliant contact model can always be applied without such limitations. Since not all of the constraints of the physical system are embodied in the rigid-body mathematical model, a study of the stability of these solutions based solely on the structure of the LCP itself is not justified. Existence and uniqueness problems suggest the inapplicability of the rigid-body model altogether and not simply uncertainty in or sensitivity to model parameter values.

Our future work addresses incorporating stability analysis as a diagnostic tool in real-time simulation where it is prudent to check for stability and warn the user in unstable regimes.

References

[1] Mirtich, B., Zhuang, Y., Goldberg, K., Craig, J., Zanutta, R., Carlisle, B., and Canny, J., 1996, ''Estimating Pose Statistics for Robotic Part Feeders,'' *Proc. of the 1996 IEEE Int'l Conf. on Robotics and Automation*, pp. 1140–1146.

[2] Donald, B. R., and Pai, D. K., 1990, ''On the Motion of Compliantly Connected Rigid Bodies in Contact: A System for Analyzing Designs for Assembly,'' *Proc. of the 1990 IEEE Int'l Conf. on Robotics and Automation*, pp. 1756–1762.

[3] Howe, R. D., and Cutkosky, M. R., 1996, ''Practical Force-Motion Models for Sliding Manipulation,'' Int. J. Robot. Res., **15**, pp. 557–572.

[4] Song, P., Yashima, M., and Kumar, V., 2000, ''Dynamic Simulation for Grasping and Whole Arm Manipulation,'' *Proc. of the 2000 IEEE Int'l Conf. on Robotics and Automation*, Vol. 2, pp. 1082–1087.

[5] Kumar, V., and Waldron, K. J., 1989, ''Actively Coordinated Vehicle Systems,'' ASME J. Mech. Des., **111**, pp. 223–231.

[6] Sacks, E., and Joskowicz, L., 1995, ''Computational Kinematic Analysis of Higher Pairs With Multiple Contacts,'' ASME J. Mech. Des., **117**, pp. 269–277.

[7] Trinkle, J., Pang, J.-S., Sudarsky, S., and Lo, G., 1997, ''On Dynamic Multi-Rigid-Body Contact Problems With Coulomb Friction,'' Z. Angew. Math. Mech., **77**, No. 4, pp. 267–280.

[8] Lötstedt, P., 1981, ''Coulomb Friction in Two-Dimensional Rigid Body Systems,'' Z. Angew. Math. Mech., **61**, pp. 605–615.

[9] Mason, M. T., and Wang, Y., 1988, ''On the Inconsistency of Rigid-Body Frictional Planar Mechanics,'' *Proc. of the 1988 IEEE Int'l Conf. on Robotics and Automation*, pp. 524–528.

[10] Wang, Y.-T., and Kumar, V., 1994, ''Simulation of Mechanical Systems With Unilateral Constraints,'' ASME J. Mech. Des., **116**, No. 2, pp. 571–580.

[11] Howard, W. S., and Kumar, V., 1993, ''A Minimum Principle for the Dynamic Analysis of Systems With Frictional Contacts,'' *Proc. of the 1993 IEEE Int'l Conf. on Robotics and Automation*, Vol. 1, pp. 437–442.

[12] Armstrong-Hélouvry, B., Dupont, P., and de Wit, C. C., 1994, ''A Survey of Models, Analysis Tools and Compensation Methods for the Control of Machines With Friction,'' Automatica, **30**, No. 7, pp. 1083–1138.

[13] Kraus, P. R., Fredriksson, A., and Kumar, V., 1997, ''Modeling of Frictional Contacts for Dynamic Simulation,'' *Proceedings of IROS 1997 Workshop on Dynamic Simulation: Methods and Applications*, Sept.

[14] Hayward, V., and Armstrong, B., 2000, ''A New Computational Model of Friction Applied to Haptic Rendering,'' *Experimental Robotics VI* (Lecture Notes in Control and Information Sciences, Vol. 250), P. Corke and J. Trevelyan, eds., Springer-Verlag, Berlin, pp. 403–412.

[15] Song, P., Kraus, P., Kumar, V., and Dupont, P., 2000, ''Analysis of Rigid Body Dynamic Models for Simulation of Systems With Frictional Contacts,'' Technical Report MS-CIS-00-08, Department of Computer and Information Science, University of Pennsylvania, available at http://www.cis.upenn.edu/~techreports.

[16] Cottle, R. W., Pang, J. S., and Stone, R. E., 1992, *The Linear Complementarity Problem*, Academic Press, San Diego, CA.

[17] Johnson, K. L., 1985, *Contact Mechanics*, Cambridge University Press, New York.

[18] Hunt, K. H., and Crossley, F. R. E., 1975, ''Coefficient of Restitution Interpreted as Damping in Vibroimpact,'' ASME J. Appl. Mech., **42**, pp. 440–445.

[19] Khalil, H. K., 1996, *Nonlinear Systems*, 2nd Ed., Prentice-Hall, Englewood Cliffs, NJ.

[20] Dupont, P. E., and Yamajako, S. P., 1997, ''Stability of Frictional Contact in Constrained Rigid-Body Dynamics,'' IEEE Trans. Rob. Autom., **13**, No. 2, pp. 230–236.

[21] McClamroch, N. H., 1989, ''A Singular Perturbation Approach to Modeling and Control of Manipulators Constrained by a Stiff Environment,'' *Proceedings of the 28th Conference on Decision and Control*, pp. 2407–2411.

[22] Oden, J. T., and Pires, E. B., 1983, ''Nonlocal and Nonlinear Friction Laws and Variational Principles for Contact Problems in Elasticity,'' ASME J. Appl. Mech., **50**, pp. 67–76.

[23] Karnopp, D., 1985, ''Computer Simulation of Stick-Slip Friction in Mechanical Dynamic Systems,'' ASME J. Dyn. Syst., Meas., Control, **107**, pp. 100–103.